

Timeliness of Wireless Sensor Networks With Random Multiple Access

Liang Li, Yunquan Dong, Chengsheng Pan, and Pingyi Fan

Abstract—In this paper, we consider a wireless sensor network in which N sensor nodes deliver the observed information of interest to a remote receiver by competing for a sharing channel through the carrier sense multiple access with collision avoidance (CSMA/CA) protocol or the slotted ALOHA protocol. For this network, we evaluate the information freshness of the two random multiple access protocols using the age of information (AoI) metric. In order to explicitly express the average AoI of the CSMA/CA based network, we establish an equivalent and tractable transmission model for the network, in which the transmission probabilities and the collision probabilities are assumed to be identical over time and among sensor nodes. For the slotted ALOHA based network, we derive the average AoI by focusing on a randomly chosen reference node. Our theoretical results show that 1) the transmission probability and collision probability of the two networks increase with both the arrival rate and the number of sensor nodes; 2) with the same transmission probability, the average AoI of the CSMA/CA based network is always smaller than that of the slotted ALOHA based network, no matter how the arrival rate and the number of nodes change. Our Monte Carlo simulation results also validate the correctness of our theoretical calculations.

Index Terms—Age of information, carrier sense multiple access with collision avoidance (CSMA/CA), random multiple access, slotted ALOHA, timely status updates.

I. INTRODUCTION

IN recent years, with the continuous development of Internet of things (IoT) technology, a growing number of emerging IoT applications appear in our daily lives, such as intelligent home, smarter healthcare, smarter city, industry 4.0 and so on [1]–[3]. In the real-time application oriented IoT systems, the remote receiver needs to perceive the physical environment and monitor the instantaneous state of the system to provide timely and effective information for intelligent decision-making and control. For example, the instantaneous

acceleration and position of vehicles in auto-driving, the temperature/soil-moisture of the ambient environment in smart agriculture, network controls of decision-making systems in modern factories of industry 4.0, and so on. For such information with timeliness requirements, delivering outdated information would reduce the reliability of system decision-making significantly and cause substantial security risks. Therefore, timeliness is essential for IoT based real-time monitoring systems and status updating systems.

Traditional data communications focus more on the delay of information transmissions. The indices such as throughput and delay could not effectively characterize the timeliness of updates. For example, in a simple M/M/1 queueing system, the more frequent the packets arrive, the larger the throughput but the delay would be out of expectation, even tends to infinity (due to congestions); the sparser the packets arrive, the fewer timely update receptions there would be, which may result in delayed information transmission and wrong action with high probability. Thus, neither delay nor throughput can exactly characterize the freshness of the received information. To this end, an emerging metric called the age of information (AoI) was formally introduced in [4]. Specifically, the AoI of the system is defined as the difference between the current moment and the generation moment of the latest successfully received update packet [5].

From the definition of AoI, we see that it is essentially different from delay and throughput and reflects accurately the freshness of the latest available information at the remote receiver. Therefore, quantifying information freshness through the AoI metric has been extensively investigated. In [5], the authors analyzed the AoI of the M/M/1, M/D/1, and D/M/1 queueing systems under the first-come-first-served (FCFS) rule through the classical queueing theory approach. Subsequently, the AoI of M/G/1 and G/G/1/1 queueing models were studied in [6] and [7], respectively. There were also some works investigating the AoI of status update systems under different service strategies, such as the last-come-first-served (LCFS) policy [8], the last-generated-first-served (LGFS) policy [9], and the zero-waiting policy (i.e., provide new information as soon as the previous one is delivered) [10]. Although the service strategies mentioned above may be suitable for certain applications, none of them is optimal in a general sense.

In wireless sensor networks (WSNs) with limited spectrum resources, packet collisions may frequently occur since multiple sensors usually access the channel over the same frequency band simultaneously. This prevents the receiver from receiving information in time and wastes many channel resources. Therefore, it is critical to utilize appropriate access protocols

Manuscript received June 19, 2022 revised March 17, 2023; approved for publication by Yin Sun, Division 3 Editor, March 25, 2023.

L. Li, Y. Dong, and C. Pan are with the School of Electronic and Information Engineering, Nanjing University of Information Science and Technology, Nanjing 210044, China, emails: {liangli, yunquandong, 003150}@nuist.edu.cn.

P. Fan is with the Beijing National Research Center for Information Science and Technology (BNRist), Beijing 100084, China. P. Fan is also with the Department of Electronic Engineering, Tsinghua University, Beijing 100084, China, email: fpy@tsinghua.edu.cn.

Part of this paper has been presented in the 2022 International Wireless Communications & Mobile Computing Conference (IWCMC 2022). The work of Y. Dong was supported by the National Natural Science Foundation of China (NSFC) under Grant 62071237. The work of C. Pan was supported by the National Natural Science Foundation of China (NSFC) under Grant 61931004. The work of P. Fan was supported by the National Key R&D Program of China under grant No.2021YFA1000500(4).

Y. Dong is the corresponding author.

Digital Object Identifier: 10.23919/JCN.2023.000014

Creative Commons Attribution-NonCommercial (CC BY-NC).

This is an Open Access article distributed under the terms of Creative Commons Attribution Non-Commercial License (<http://creativecommons.org/licenses/by-nc/3.0>) which permits unrestricted non-commercial use, distribution, and reproduction in any medium, provided that the original work is properly cited.

so that multiple sensors can efficiently deliver their monitored status updates over a shared channel. Moreover, since for the networks with a large number of sensors, each sensor may work intermittently, the fixed multiple access techniques like time division multiple access (TDMA) and frequency division multiple access (FDMA) may not be suitable for such scenarios and with low efficiency. Thus, random multiple access techniques, (e.g., carrier sense multiple access with collision avoidance (CSMA/CA) and slotted ALOHA and so on) are the promising modes for WSNs.

The CSMA/CA and the slotted ALOHA have been extensively investigated in terms of traditional performance metrics such as throughput and delay. For instance, in [11], G.Bianchi analyzed the throughput of a CSMA/CA based network by employing a two-dimensional Markov chain model. However, the model proposed by G.Bianchi is only applicable to saturated networks, i.e., all the nodes have data packets to transmit all the time. Thus, Duffy *et al.* have extended this Markov chain model to the unsaturated networks [12]. Slotted ALOHA stability has been studied in [13] and [14]. In [13], the authors studied the stability region for a finite user infinite cache in a slotted ALOHA system. The authors gave the precise region of system stability for the two-user case. Along a similar line, the authors in [14] analyzed the stability of the system in the case of infinite users with single buffer. The results of the drift analysis showed that when the number of users approaches infinity, the Markov chain of the channel backlog is ergodic in a collision channel if the packet rate is smaller than the expected number of successfully received packets.

There have been some works investigating the AoI for CSMA based networks, such as [4] and [15]–[19]. To be specific, in [4], the average AoI of a CSMA based vehicular network is investigated through simulations. In [17], the authors used the stochastic hybrid systems technology to analyze the AoI of the CSMA based network under the condition that no collisions occur and the channel perception delay is zero. They also derived the average AoI of a CSMA based network with a large collision probability in [18]. In our previous work, the average AoI a CSMA/CA based network was analyzed theoretically [19]. There were several applications of CSMA in CSMA based IoT LoRa networks, such as the wildlife state monitoring in transmission LoRa networks [20] and the remote sensor data transmission in IoT LoRa network [21].

For the ALOHA based networks, the information freshness was explored in [22]–[28]. Particularly, the average AoI of a slotted ALOHA-like network with all-active source nodes (i.e., generating data packets in every slot) was investigated in [22]. In [23], it analyzed the AoI of a slotted ALOHA based network with an infinite number of source nodes. To be specific, they proposed a dynamically packets discarding scheme to minimize the average AoI of the network, which may be suitable to those time sensitive scenarios. In [24], the authors studied several scheduling strategies for a multi-access channel. They optimized the AoI of the network under the requirement of satisfying the real-time throughput of each node. In random access applications, however, adopting such strategies would consume a lot of communication. The age of an unslotted, uncoordinated, and unreliable multi-access

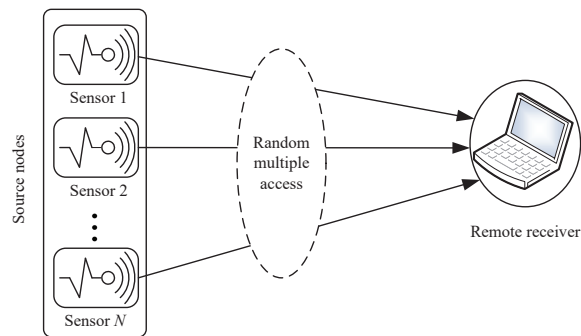


Fig. 1. The wireless sensor network model, in which N sensors share a common channel through the CSMA/CA or the slotted ALOHA protocol.

collision channel was analyzed in [25]. The results showed that when the number of nodes and the update rate increase with a constant proportion, the limiting asymptotic age can denote as an approximation age for each node. The information age of the feedback-free slotted ALOHA transmission system using retransmission strategy has been investigated in [26]. It found that for low arrival rates, the retransmission strategy can diminish the message age with a cost of throughput. An age threshold based ALOHA protocol was proposed in [27], in which every node is allowed to access the channel with a certain probability only if its immediate AoI is larger than a predefined age threshold. The joint optimization of the transmission probability and the age threshold was investigated in [28]. They found that the optimal AoI is $1.4169n$ times the network size n . In practical engineering implementations, ALOHA has also been selected as the multiple access technique for the low power wide area networks (LPWAN) [29]–[31].

However, the aforementioned works neither provided explicitly expressions of average AoI for CSMA/CA based network nor provided a comparison on their timeliness. In this paper, we try to discuss these two issues. The target of us is that explicitly characterize the timeliness of an unsaturated wireless sensor network in terms of AoI, for the CSMA/CA protocol and the slotted ALOHA (shown in Fig. 1). The main difference from those previous works described above is that we set up an equivalent and tractable transmission model to evaluate the AoI performance explicitly, and the results can reflect the system parameters precisely.

A. Main Contributions

The contributions of this paper are summarized as follows.

- 1) For the CSMA/CA based network, we develop an equivalent and universal transmission model for the transmission process and back-off process. Based on this newly developed model, we derive the transmission probability and the collision probability of the sensor nodes explicitly. In the slotted ALOHA based network, we also derive the transmission probability and the collision probability of the sensor nodes explicitly. We show that both the transmission probability and the collision probability are

increasing with the arrival rate and the number of sensor nodes.

- 2) For both the CSMA/CA based and the slotted ALOHA based networks, we derive the maximum packet rates and the allowable numbers of sensor nodes. We also explicitly present the average AoIs of two networks in closed forms. Our results show that the average AoI of the CSMA/CA based network is always smaller than that of the slotted ALOHA based network for the same transmission probability, regardless of changes in the arrival rate and the number of sensor nodes. To the best knowledge of the authors, this is the first result explaining why the CSMA/CA outperforms the slotted ALOHA in terms of AoI in theory.
- 3) We investigate the transmission probability, the collision probability, and the average AoIs of heterogeneous networks through simulations. The simulation results indicate that the changes in the transmission probability, the collision probability, and the average AoIs are with similar modes to the corresponding homogeneous networks.

B. Organization

The rest of the paper is organized as follows. We present the wireless sensor network model and the definition of the AoI in Section II. In Section III, we analyze the CSMA/CA and the slotted ALOHA transmission behaviors and establish an equivalent and universal transmission model for the CSMA/CA based network to derive the transmission probability and collision probability of the sensor nodes. We also explicitly obtain closed-form expressions for the average AoIs of networks that employ the CSMA/CA protocol and the slotted ALOHA protocol. The Monte Carlo simulation results and numerical results are given in Section IV. Finally, the conclusion and future direction are presented in Section V.

II. SYSTEM MODEL

As shown in Fig. 1, we consider a single-hop wireless sensor network consisting of N identical sensor nodes and a common remote receiver, in which all sensor nodes are visible to each other (i.e., without hidden nodes). Each sensor node observes the information of interest and attempts to transmit the observed information to the remote common receiver independently. All the sensor nodes contend for the channel through the CSMA/CA protocol or the slotted ALOHA protocol. We assume that the data packet generation of each sensor node follows the Bernoulli process with a rate of p . Every sensor node stores its data packets in a buffer and delivers the data packets using the FCFS policy.

Time is divided into discrete slots of equal length and all data packets are of the same size. The start and completion of each data packet transmission occur at the slot boundaries and it takes exactly one slot for the transmission of every data packet. We assume that transmission failures occur only when two or more nodes are transmitting their data packets in the same slot. In addition, we employ the late-arriving system

with delayed access. That is, the data packets are generated or received at the end of slots.

In a slotted CSMA/CA based network, every sensor node needs to wait for a random period of t slots (which is referred to as the back-off time) before attempting to transmit a data packet to avoid collisions. The back-off time t would be chosen uniformly from $(0, 1, \dots, w_s)$, where $w_s = 2^s w_0$, w_0 is the minimum contention window, and s is the number of previous failed back-off stage. We assume that the number of back-offs can be infinite (i.e., $s = 0, 1, \dots$). The initial back-off time t of a sensor node is recorded by its back-off counter, which would be reduced by one in each slot if all other sensor nodes are silent. Otherwise, it remains unchanged. When the back-off counter reaches zero, a sensor node has the opportunity to transmit its head-of-line packet. If the transmission is successful, the sensor node could start the back-off process of a new data packet by resetting its back-off stage s to zero and resetting its back-off counter randomly between zero and $w_0 - 1$. If a collision occurs, the sensor node enters the next back-off stage by doubling the contention window and initializing the back-off counter. We refer to the number of previous failed back-offs and the back-off counter of a sensor node as its state, which is denoted as (s, t) .

In a slotted ALOHA based network, to reduce the randomness of sensor nodes transmitting their data packets, and sensor nodes must wait until the next slot before they can start delivering their data packets. In particular, every data packet would be transmitted with the same transmission probability λ in each slot. If any collisions occur, the data packet would be retransmitted with probability λ in the next slot, until the transmission is successful.

In this paper, both the CSMA and ALOHA protocols that we consider are slotted protocols. For the CSMA protocol, a node attempts to transmit its packet when its back-off counter reduces to zero. In case a collision occurs, the node needs to perform a new round of back-off process (cf. Section III-A). For the slotted ALOHA protocol, each node delivers its packet with a certain probability λ and retransmits the packet with the same probability when a collision occurs.

We evaluate the timeliness of the network by the AoI. To be specific, the AoI is defined as the difference between the current time m and the generation time $U_n(m)$ of the latest successfully transmitted packet at sensor node n . Mathematically, the AoI is expressed as

$$\Delta_n(m) = m - U_n(m). \quad (1)$$

Fig. 2 describes a sample AoI path $\Delta(m)$ of a certain sensor node n . We denote the generation (arrival) time of the k th packet status update of the sensor node as m_k ($k = 1, 2, \dots$) and the time when the remote receiver receives the k -th packet of a sensor node n as m'_k . Then the inter-arrival time of the packets can be expressed as $X_k = m_k - m_{k-1}$ and the system time of k th packet is $T_k = m_k - m'_k$. The waiting time and the service time of packet k are denoted, respectively, as W_k and S_k . It is noted that the system time T_k of packet k is the sum of the waiting time W_k and the service time S_k . Thus

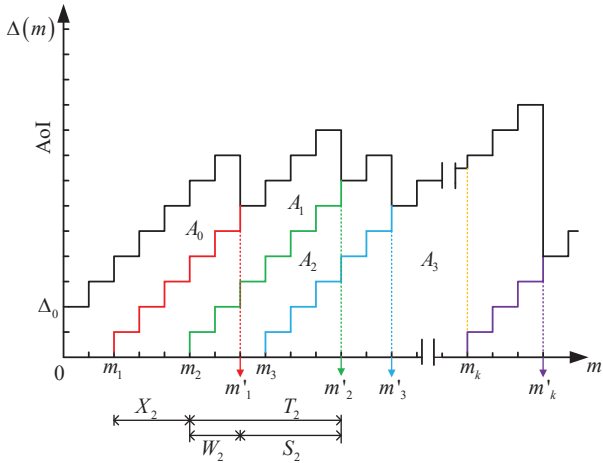


Fig. 2. A sample path of the AoI.

we have

$$T_k = W_k + S_k. \quad (2)$$

Without loss of generality, it is supposed that the system is observed from $m = 0$. At this moment, the queues are empty and the AoI at the remote receiver is Δ_0 . Between time m'_{k-1} and time m'_k , the AoI is increased by one since the remote receiver does not receive a new data packet from sensor node n . Once the remote receiver receives an update (a data packet) from a sensor node n , the AoI of the sensor node is reset to a lower value which is equal to the latency experienced by the data packet across the transmission system.

We assume that the packet arrival process and the age process $\Delta(m)$ are ergodic. Thus, we know that the sample average AoI converges to its statistical average. During a period of M slots, we assume that K packets are successfully received by the remote receiver. Then the average AoI, in the period, can be expressed as

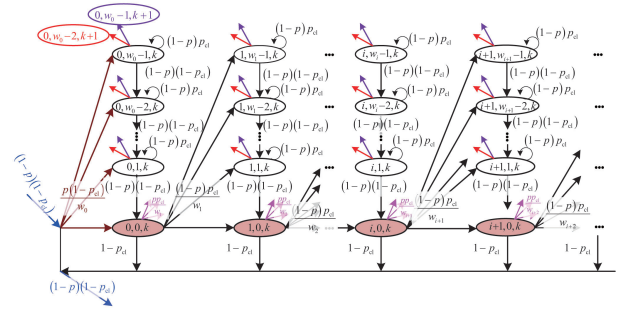
$$\bar{\Delta} = \frac{1}{M} \sum_{m=1}^M \Delta(m). \quad (3)$$

To calculate this average, the area $\Delta(m)$ shown in Fig. 2 is divided into a sequence of triangle-like areas A_0, A_1, A_2, \dots , and the triangle-like area with width T_K . As M approaches infinity, the average AoI can be expressed as

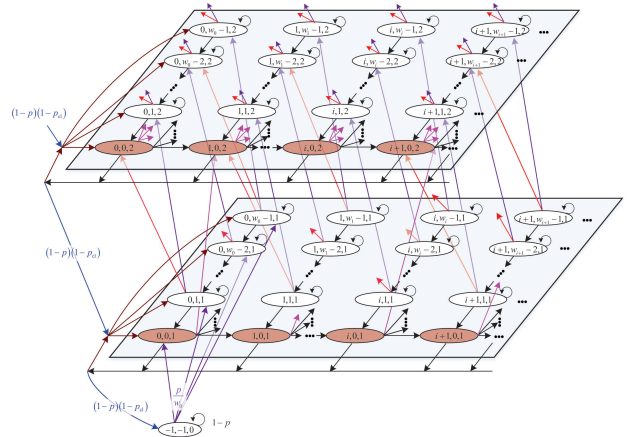
$$\bar{\Delta} = \lim_{M \rightarrow \infty} \frac{1}{M} \left(A_0 + \sum_{k=1}^{K-1} A_k + \frac{1}{2} T_K (T_K + 1) \right). \quad (4)$$

III. TRANSMISSION BEHAVIOR AND AVERAGE AOI OF CSMA/CA AND SLOTTED ALOHA BASED NETWORKS

In this section, we first develop an equivalent transmission model for the network using the slotted CSMA/CA protocol. Based on the newly developed model, we derive the transmission probability, the collision probability, and the service rate of the sensor nodes. Likewise, in the slotted ALOHA based network, we also analyze the transmission probability,



(a) Transition diagram for each sensor node buffer size $c = k \geq 1$



(b) Transition diagram of the three-dimensional Markov chain

Fig. 3. Three dimensional transition diagram for a sensor node state (s, t, c) .

the collision probability, and the service rate of the sensor nodes. After that, the maximum arrival rate and the number of sensor nodes allowed by the network are calculated. Finally, we derive the average AoI of the CSMA/CA based network and the slotted ALOHA based network explicitly.

A. Equivalent Transmission Model of the CSMA/CA Network

Since the transmission behavior of the CSMA/CA protocol is quite complex, we shall establish an equivalent and universal transmission model to facilitate the analysis of the transmitting process.

Motivated by the approximation method proposed by G. Bianchi in [11], we assume that for each transmission, the collision probability p_{cl} is identical and independent among sensor nodes, regardless of the number of retransmissions experienced. In each slot, every sensor node having a non-empty buffer transmits its data packets with transmission probability p_{tx} , which is also identical and independent, regardless of its back-off state. For every sensor node, therefore, p_{cl} is the probability that the transmission of a sensor node collides with some other sensor nodes; p_{tx} is the probability that the back-off counter of the sensor node reduces to zero and attempts to transmit a data packet.

We refer to the number s of failed back-offs, the back-off counter t of a sensor node, the number c of packets in the

cache as the state of the sensor node, and thus model the three-dimensional process (s, t, c) as a discrete-time Markov chain. In addition, we assume that the number of back-off stages can be infinite. Unlike the research of in [11], however, we shall investigate the network in the non-saturated case in this paper. That is, the buffer of all sensor nodes is not always non-empty, and thus is more meaningful for systems with strict timeliness requirements. In particular, we say a sensor node is in the idle state $(-1, -1, 0)$ if its buffer is empty, i.e., $c = 0$.

The three-dimensional state (s, t, c) transition diagram of the discrete-time Markov chain is shown in Fig. 3, in which Fig. 3(a) describes the state transitions when the buffer length is $c = k \geq 1$ is not changed by a step of transition. Fig. 3(b) describes possible transitions between neighboring layers, i.e., the buffer length is increased or decreased by one. In particular, the non-zero one-step transition probabilities of the k th layer corresponding to Fig. 3(a) are given by:

$$\begin{cases} \Pr\{i, j, k | i, j, k\} = (1-p)p_{cl} \\ \Pr\{i, j-1, k | i, j, k\} = (1-p)(1-p_{cl}) \\ \Pr\{0, j, k | i, 0, k\} = \frac{p(1-p_{cl})}{w_0} \\ \Pr\{i+1, j, k | i, 0, k\} = \frac{(1-p)p_{cl}}{w_{i+1}}, \end{cases} \quad (5)$$

in which p is the data packet generation rate of each sensor node, $i = 0, 1, \dots, j \in (1, w_i - 1)$, and $k \geq 1$.

In (5), the first equation and the second equation account for the situations that no data packet is generated. In this case, the back-off counter will be frozen if a collision is detected and will be decremented by one if no collision occurs, respectively. The third equation models situations when the back-off counter returns to zero. To be specific, if a sensor node transmits its data packet without any collisions (the data packet is removed from the buffer) and generates a new data packet in the slot (the new data packet is pushed into the buffer), the sensor node will start a new back-off process in the same layer. Finally, the fourth equation models the situation that the sensor node will go to the next back-off stage $i+1$ in the same layer and initial the back-off counter value (which is chosen between zero and $w_{i+1} - 1$), if a collision is detected at the i th back-off stage and no data packet arrives.

When the number c of data packets in the buffer changes, the state transition diagram of the discrete-time Markov chain is shown in Fig. 3(b) and the non-zero transition probabilities are as follows:

$$\begin{cases} \Pr\{-1, -1, 0 | -1, -1, 0\} = 1-p \\ \Pr\{0, j, 1 | -1, -1, 0\} = \frac{p}{w_0} \\ \Pr\{-1, -1, 0 | i, 0, 1\} = (1-p)(1-p_{cl}) \\ \Pr\{0, j, k | i, 0, k\} = \frac{(1-p)(1-p_{cl})}{w_0} & k \geq 2 \\ \Pr\{i+1, j, k+1 | i, 0, k\} = \frac{pp_{cl}}{w_{i+1}} & k \geq 1 \\ \Pr\{i, j, k+1 | i, j, k\} = pp_{cl} & k \geq 1 \\ \Pr\{i, j-1, k+1 | i, j, k\} = p(1-p_{cl}) & k \geq 1. \end{cases} \quad (6)$$

The first equation in (6) accounts for the situation that when the buffer is empty and no data packet is generated in the slot. The second equation characterizes the case that the sensor node generates a data packet and will transit to the zeroth back-off stage by randomly initializing the back-off counter. The third equation describes the case when the sensor node successfully delivers its only ($k = 1$) data packet, and no new data packet arrives. Likewise, the fourth equation of (6) accounts for the situation that when the sensor node successfully transmits its head-of-line packet ($k \geq 2$) and no new data packet arrives. In this case, the back-off process of the followed data packet restarts from the next layer. The fifth equation characterizes the case when the back-off counter at the i th back-off stage of the k th layer returns to zero and a collision is sensed, simultaneously, the sensor node gets a new data packet. Thus, the state will be transferred to the next back-off stage $i+1$ of the $k+1$ th layer. Finally, as shown in the sixth equation and the seventh equation of (6), the back-off counter is non-zero and the sensor node gets a new data packet.

We represent the stationary distribution of the Markov chain as $b_{i,j,k} = \lim_{m \rightarrow \infty} \Pr\{(s, t, c) = (i, j, k)\}$. We also denote $b_{i,j,*} = \sum_{k=1}^{\infty} b_{i,j,k}$. In the stationary state, for each sensor node, the state update rate (i.e., the rate of packet generation) is p , and we further represent the service rate of the network using the CSMA/CA protocol as μ_{CA} . In particular, the stationary distribution \mathbf{b} is explicitly given in the following proposition.

Proposition 1. Given the packet rate p and the collision probability p_{cl} , the stationary distribution of the three-dimensional Markov chain can be expressed as

$$b_{0,0,*} = p, \quad (7)$$

$$b_{i,0,*} = pp_{cl}^i, \quad (8)$$

$$b_{i,j,*} = \frac{p(w_i - i)p_{cl}^i}{w_i(1-p_{cl})}, \quad (9)$$

$$b_{-1} = 1 - \frac{p(4p_{cl}^2 - (w_0 + 4)p_{cl} + w_0 + 1)}{2(1-p_{cl})^2(1-2p_{cl})}, \quad (10)$$

in which $i \geq 1, 0 \leq j \leq w_i - 1$, and $w_i = 2^i w_0$. Moreover, the idle probability of the sensor nodes is given by

$$p_{idle} = b_{-1}. \quad (11)$$

Proof. Since all the states are connected and the Markov chain is irreducible, the Markov chain has a unique stationary distribution. More details are shown in Appendix A. ■

According to the stationary distribution of the Markov chain acquired in Proposition 1, we can get the transmission probability p_{tx} and the collision probability p_{cl} of the sensor nodes, as shown in the following theorem.

Theorem 1. Given the packet rate p and the stationary distribution \mathbf{b} of the Markov chain, the transmission probability p_{tx} and the collision probability p_{cl} of the sensor nodes in the network satisfies

$$p_{tx} = \frac{p}{1-p_{cl}}, \quad (12)$$

$$p_{cl} = 1 - (1 - p_{tx})^{N-1}, \quad (13)$$

in which N is the number of sensor nodes.

Proof. Note that a sensor node attempts to transmit its data packets every time when its back-off counter value is equal to zero. Therefore, the transmission probability p_{tx} is the total probability that the sensor node is in state $(i, 0, k)$, in which all $i \geq 0$, $k \geq 1$. The collision probability p_{cl} is the conditional probability that when a certain sensor node attempts to transmit its data packets, while at least having an interfering node transmits its data packets. Please refer to Appendix B for a detailed proof. ■

According to (12) and (13), we further have the following expression about the collision probability p_{cl}

$$f(p_{cl}) = 1 - p_{cl} - \left(1 - \frac{p}{1 - p_{cl}}\right)^{N-1} = 0. \quad (14)$$

Since (14) is a nonlinear equation, we solve the collision probability p_{cl} with Newton's iteration method by iteratively using $p_{cl} = p_{cl} - f(p_{cl})/f'(p_{cl})$, starting from an initial value close to zero. The algorithm is shown in Algorithm 1. The proof of convergence of Newton's iterative method can be found in [32, Chap. 7.4]. From Algorithm 1, we can obtain

Algorithm 1 Solving for the collision probability p_{cl}

1: **Input:** Packet rate p , the number of node N , and tolerable iterative error ϵ
2: **Output:** p_{cl} : Collision probability
3: **Initialize:** $p_{cl}^{(0)}$
4: **while:** $\Delta > \epsilon$, **do**
5: $i = i + 1$
6: Calculate $p_{cl}^{(i)} = p_{cl}^{(i-1)} - f(p_{cl}^{(i-1)})/f'(p_{cl}^{(i-1)})$
7: Calculate $\Delta = |p_{cl}^{(i)} - p_{cl}^{(i-1)}|$
8: Let $p_{cl} = p_{cl}^{(i)}$
9: **End While**

the collision probability p_{cl} . The transmission probability p_{tx} and the idle probability p_{idle} can also be acquired by using (12) and (11), respectively.

It is worth noting that a sensor node can transmit the data packet successfully in each slot only if the node gets the chance to use the channel and no collision occurs. Therefore, the probability of a sensor node successfully delivering a data packet in each slot can be expressed as

$$p_s = p_{tx}(1 - p_{cl}) = p. \quad (15)$$

Accordingly, we can obtain the service rate of a sensor node of the network using the CSMA/CA protocol as follows

$$\mu_{CA} = \frac{p}{1 - p_{idle}}. \quad (16)$$

We denote the time at which a sensor node successfully transmits a data packet as the service time S_k and model the service time S_k as a geometric distribution with parameter μ_{CA} . That is,

$$\Pr\{S_k = j\} = \mu_{CA}(1 - \mu_{CA})^{j-1}, j = 1, 2, \dots \quad (17)$$

Further, the average service time can be represented as

$$\mathbb{E}[S_k] = \frac{1}{\mu_{CA}}. \quad (18)$$

Equation (17) can be interpreted as follows. In each slot of the transmission, the service would be completed with probability μ_{CA} at the end of that slot and would be continued in the next slot with probability $1 - \mu_{CA}$.

Remark 1. Under the condition that the packet rate approaches the service rate, i.e., $p \rightarrow \mu_{CA}$, we have $p_{idle} \rightarrow 0$ from (16).

- Given the number N of sensor nodes, for each stable buffer, the packet rate must satisfy $p < \mu_{CA}$. Since μ_{CA} is in fact a function of p , we can find the maximum achievable packet rate p_{max} in the process $p \rightarrow \mu_{CA}$, for which we have $p_{idle} = 0$ from (16). From the expression (11) of p_{idle} and by combining (13) to (11), we have

$$\frac{p_{tx}(4p_{cl}^2 - (w_0 + 4)p_{cl} + w_0 + 1)}{2(1 - p_{tx})^{N-1}(1 - 2p_{cl})} = 1, \quad (19)$$

in which $p_{cl} = 1 - (1 - p_{tx})^{N-1}$. In particular, we can solve p_{tx} from (19) by using some mathematical tools (e.g., Matlab). We denote the real solution of p_{tx} is denoted as $\overline{p_{tx}}$ and know that $\overline{p_{tx}}$ is the maximum transmission probability. By substituting (13) into (12) and replacing p_{tx} with $\overline{p_{tx}}$, the maximum packet rate can be expressed as

$$p_{max} = \overline{p_{tx}}(1 - \overline{p_{tx}})^{N-1}. \quad (20)$$

- Likewise, for a fixed packet rate and a varying N , the idle probability p_{idle} also approaches zero as N approaches the maximum available number N_{max} of the system. Thus, we have

$$\frac{p(4p_{cl}^2 - (w_0 + 4)p_{cl} + w_0 + 1)}{2(1 - p_{cl})^2(1 - 2p_{cl})} = 1. \quad (21)$$

By expressing p_{tx} in terms of p_{cl} (cf. (13)) and solving p_{cl} from (21) (denoting the real solution of p_{cl} as $\overline{p_{cl}}$), N_{max} can be then expressed as

$$N_{max} = \left\lfloor \frac{\ln(1 - \overline{p_{cl}})}{\ln(1 - p_{tx})} + 1 \right\rfloor, \quad (22)$$

in which $\lfloor x \rfloor$ represents the largest integer not exceeding x .

B. Transmissions of the Slotted ALOHA Based Network

In the slotted ALOHA based network, we refer to a certain sensor node arbitrarily selected from the N sensor nodes as the reference node while referring to the remaining $N - 1$ sensor nodes except the reference node as the other nodes.

To evaluate the interference of the other nodes on the reference node, we need to know the busy probability p_{bsy} of the other nodes. Specifically, a sensor node is said to be in the busy state if its buffer is not empty and in the idle state otherwise. Thus, the idle probability p_{idl} and the busy probability p_{bsy} of a sensor node satisfies $p_{idl} + p_{bsy} = 1$.

It is clear that an idle sensor node will not crowd the channel. Only when a sensor node is in busy state, the sensor node would compete for the channel. The busy probability p_{bsy} and (re)transmission probability λ of a sensor node, therefore, have a decisive effect on crowdedness of the channel.

When the reference node performs a data packet transmission in a given slot, the probability p_s of successful transmission can be expressed as

$$p_s = (1 - p_{tx})^{N-1}, \quad (23)$$

in which $p_{tx} = \lambda p_{bsy}$ is the probability that there is a data packet(s) in the buffer of the other nodes and the head-of-line data packet is transmitted with probability λ . When the reference node decides to deliver a data packet in the current slot, a collision occurs as long as one or more of the other nodes attempt to transmit their data packets.

According to (23), therefore, the collision probability p_{cl} can be expressed as

$$\begin{aligned} p_{cl} &= 1 - p_s = 1 - (1 - p_{tx})^{N-1} \\ &= 1 - (1 - \lambda p_{bsy})^{N-1}. \end{aligned} \quad (24)$$

Specifically, $1 - p_{tx}$ is the probability that one of the other node has a data packet(s) but does not attempt to transmit a data packet and $(1 - p_{tx})^{N-1}$ is the probability that none of the other $N - 1$ nodes are transmitting. Thus, $1 - (1 - p_{tx})^{N-1}$ is the probability that at least one of the other $N - 1$ nodes try to transmit its data packet and collides with the reference node.

In each slot, every busy node would transmit their data packets with probability λ . The node could successfully deliver its update only if the node obtains the right to use the channel and there is no collision. Therefore, the probability of successful transmission can be expressed as

$$\begin{aligned} \mu_{SA} &= \lambda(1 - p_{cl}) = \lambda(1 - p_{tx})^{N-1} \\ &= \lambda(1 - \lambda p_{bsy})^{N-1}, \end{aligned} \quad (25)$$

which is referred to as the service rate of the slotted ALOHA based network.

We denote the time for the reference node to successfully deliver an update k as S_k . It is clear that the service time S_k is a geometrically distributed random variable with parameter μ_{SA} . Therefore, the probability distribution of the service time and the average service time can be, respectively, written as

$$\Pr\{S_k = j\} = \mu_{SA}(1 - \mu_{SA})^{j-1}, \quad j = 1, 2, \dots, \quad (26)$$

$$\mathbb{E}[S_k] = \frac{1}{\mu_{SA}}. \quad (27)$$

To solve the unknown variable p_{bsy} , we shall model the buffer state (i.e., the number of data packets in the buffer) of the reference node as a discrete-time Markov chain of which the state transition diagram is shown in Fig. 4.

Further, the steady-state probability distribution of the discrete-time Markov chain is given by the following proposition.

Proposition 2. The steady-state probability for the buffer state of the reference node being empty is given by

$$b_0 = \frac{\mu_{SA} - p}{\mu_{SA}} = 1 - \frac{p}{\mu_{SA}}. \quad (28)$$

Proof. See Appendix C. ■

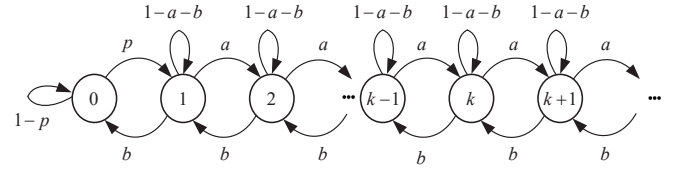


Fig. 4. Discrete-time Markov chain state transition diagram of the reference node, in which $\bar{p} = 1 - p$, $\mu_{SA} = 1 - \mu_{SA}$, $a = p\mu_{SA}$, and $b = \mu_{SA}\bar{p}$.

Algorithm 2 Solving for the busy probability p_{bsy}

1: **Input:** Packet rate p , the transmission probability λ , and tolerable iterative error ϵ
 2: **Output:** p_{bsy} : Busy probability
 3: **Initialize:** $p_{bsy}^{(0)}$
 4: **While:** $\Delta > \epsilon$, **do**
 5: $i = i + 1$
 6: Calculate $p_{bsy}^{(i)} = p_{bsy}^{(i-1)} - f(p_{bsy}^{(i-1)})/f'(p_{bsy}^{(i-1)})$
 7: Calculate $\Delta = |p_{bsy}^{(i)} - p_{bsy}^{(i-1)}|$
 8: Let $p_{bsy} = p_{bsy}^{(i)}$
 9: **End While**

Note that p_{idl} is the probability that the buffer of the reference node is empty. Based on the Proposition 2, we have

$$p_{idl} = b_0 = 1 - \frac{p}{\mu_{SA}}. \quad (29)$$

Further, by combining $p_{idl} + p_{bsy} = 1$ with (29), we have

$$p_{bsy} = \frac{p}{\mu_{SA}}. \quad (30)$$

By substituting (30) into (25), we have the following equation on the busy probability p_{bsy}

$$f(p_{bsy}) = \frac{p}{p_{bsy}} - \lambda(1 - \lambda p_{bsy}) = 0. \quad (31)$$

We employ Newton's iteration method with $p_{bsy} = p_{bsy} - f(p_{bsy})/f'(p_{bsy})$ and an initial value $p_{bsy}^{(0)}$ to solve the numerical solution of the busy probability p_{bsy} . We can find a detailed proof of the convergence of Newton's iteration method in [32, Chap. 7.4]. The numerical solution of the busy probability p_{bsy} is shown in Algorithm 2. Moreover, we can obtain the update service rate μ_{SA} and the collision probability p_{cl} by (25) and (24), respectively.

Remark 2. In order to obtain the maximum data packet rate p_{max} and the maximum allowable number of sensor nodes N_{max} in the slotted ALOHA based network, we set the data packet rate to be close to the service rate (i.e., $p \rightarrow \mu_{SA}$) for a fixed (re)transmission probability λ of each sensor node. In this cases, we have $p_{bsy} \rightarrow 1$ (cf. (30)). For each stable buffer, the packet rate must satisfy $p < \mu_{SA}$.

- Given the number N of sensor nodes, by combining (25), we can get approximately the maximum packet rate as follows:

$$p_{max} = \lambda(1 - \lambda)^{N-1}. \quad (32)$$

- Given the packet rate p , according to (25), the maximum

allowable number of sensor nodes can be expressed by

$$N_{\max} = \left\lfloor \frac{\ln \frac{p}{\lambda}}{\ln(1-\lambda)} + 1 \right\rfloor, \quad (33)$$

in which $\lfloor x \rfloor$ denotes the largest integer that is not greater than x .

C. Average AoI of the Networks

For each node, we note that the arrival of data packets follows the Bernoulli process with the parameter p and the service time S_k obeys the geometric distribution with the parameter μ . Thus, the transmission process of each node can be modeled by a Geom/Geom/1 queue. Moreover, we model the queuing process as a late-arriving system with delayed access. Under this model, the probability generating function (PGF) of the system time T_k of a packet is given by the following lemma.

Lemma 1. For a given the data packet arrival rate p , the PGF of the system time T_k is given by

$$G_T(z) = \frac{\beta z}{1 - (1 - \beta)z}, \quad (34)$$

in which

$$\beta = \frac{\mu - p}{1 - p}. \quad (35)$$

Proof. A detailed proof of the probability generation function of the system time T_k of the Geom/Geom/1 queuing model can be found in [33, Chap. 3.1.2]. ■

Equation (34) shows that the system time T_k obeys the geometric distribution of parameter β . Thus, the probability distribution of the system time and the average system time of data packets are expressed, respectively, as

$$\Pr\{T_k = j\} = \beta(1 - \beta)^{j-1}, \quad j \geq 1, \quad (36)$$

$$\mathbb{E}[T_k] = \frac{1}{\beta}. \quad (37)$$

Based on this Geom/Geom/1 queuing model, the average AoI of the network can be obtained, which is given by the following theorem.

Theorem 2. Given the generation rate p of data packets, the average AoI of the network is given as follows:

$$\bar{\Delta} = \frac{1}{p} + \frac{p}{\mu} + \frac{1-p}{\mu-p} - \frac{p}{\mu^2}. \quad (38)$$

Proof. See Appendix D. ■

From Theorem 2, we can obtain the average AoIs of the two networks using the CSMA/CA protocol and the slotted ALOHA protocol, in which the service rate μ are given, respectively, by (16) and (25).

In the following, we study two extreme cases of the network using two random multiple access strategies and obtain the subsequent results.

First, as the generation rate of data packets approaches zero (i.e., $p \rightarrow 0$), according to (39), it is clear that the average AoIs of the network goes to infinity.

In this situation, due to the sparse arrival of data packets, the shared channel is rarely occupied by transmissions and the inter-arrival time would be large. Therefore, in most circumstances, the data packets received by the remote receiver are not fresh.

Second, when the packet generation rate reaches the maximum allowable packet rate (i.e., $p \rightarrow p_{\max}$, at this time, $p_{\max} \rightarrow \mu$), it is seen from (39) that the average AoIs of the network also is infinity.

In this situation, since the high packet arrival rate leads to frequent collisions occurring, the shared channel is always congested. Therefore, the service time of the data packet may be arbitrarily long, making the average AoIs infinite.

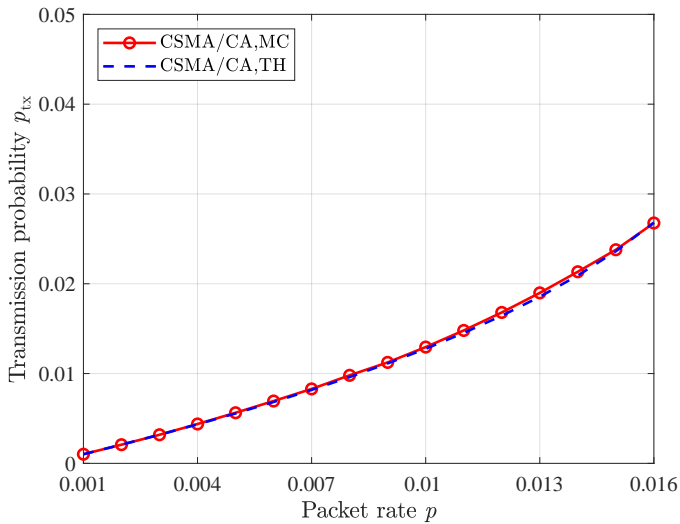
IV. SIMULATION RESULTS

In this section, we investigate the average AoI of the networks via the numerical and the Monte Carlo simulation results. We set the minimum competition window as $w_0 = 8$. We assume that both the networks using the CSMA/CA and slotted ALOHA protocols are homogeneous. That means that the packet rates of all the nodes are the same. For the fairness of comparison, we also ensure that the transmission probability p_{tx} of the network employing the CSMA/CA protocol and the slotted ALOHA protocol are *equal*, which can be realized by adjusting the (re)transmission probability λ .

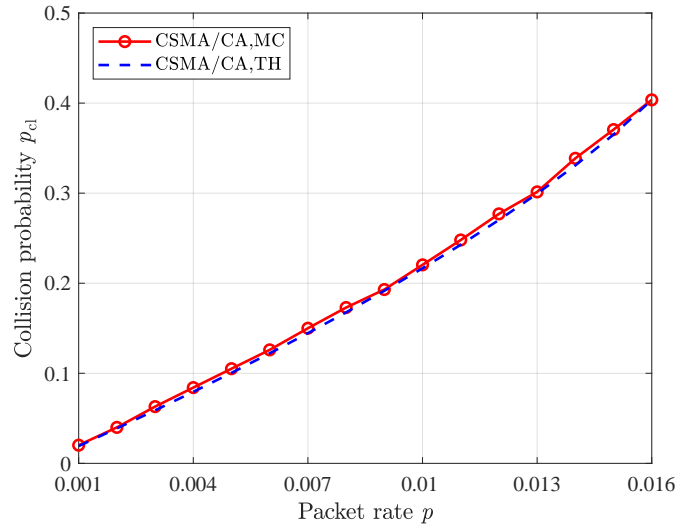
First, we observe from Figs. 5(a) and 5(b) that the transmission probabilities p_{tx} of the networks using the CSMA/CA protocol is increasing with both the packet rate p and the number N of nodes. This is because the increase in packet rate p leads to a larger probability of non-empty buffer, which further leads to a larger transmission probability p_{tx} . Likewise, an increase in the number of nodes leads to more attempts of transmitting and thus a larger transmission probability p_{tx} . It is also observed in Fig. 5(a) and Fig. 5(b) that the Monte Carlo simulation (MC) results match our theoretical results (TH) very well.

It is observed from Fig. 6(a) and Fig. 6(b) that the collision probability p_{cl} of the networks using the CSMA/CA protocol increases with the packet rate p and the number N of nodes. This is because as the packet rate and the number N of nodes increases, there will be more contentions in the transmissions. Moreover, according to the derivations, we also find that with packet rate and the number of nodes increase both transmission and collision probabilities increase in polynomial with an order of three.

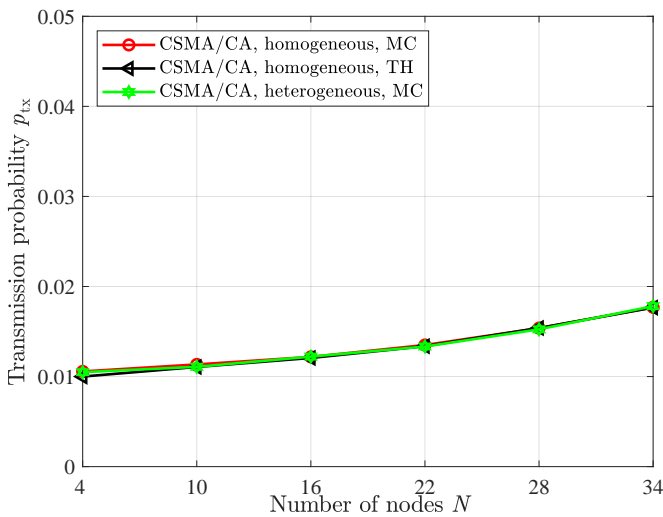
In Fig. 7(a), we show how the average AoIs of the CSMA/CA and slotted ALOHA based networks varies with the packet rate p , in which the number of sensor nodes is set to $N = 20$. First, we observe that as the packet rate p increases, the average AoI is decreasing first and then increasing. When the packet rate p is relatively small or large, the average AoIs are quite large. This is because the waiting time for the new updates are large when the packet rate is small while collisions occur more frequently and thus the service time is larger when the packet rate is large. Second, for the CSMA/CA based network, the average AoI reaches the minimum when the packet rate p is close to 0.014; in the



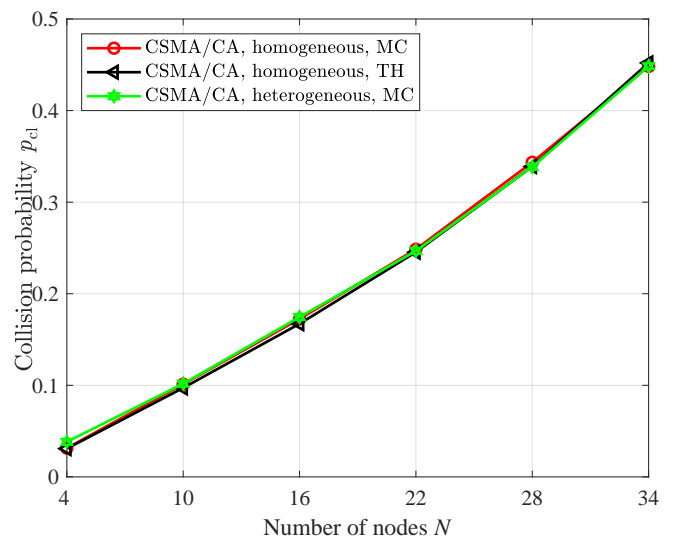
(a) Transmission probability p_{tx} versus the packet rate p ($N = 20$)



(a) Collision probability p_{cl} versus the packet rate p ($N = 20$)



(b) Transmission probability p_{tx} versus the number of nodes N ($p = 0.01$)



(b) Collision probability p_{cl} versus the number of nodes N ($p = 0.01$)

Fig. 5. Change in the transmission probability p_{tx} .

Fig. 6. Change in the collision probability p_{cl} .

slotted ALOHA based network, the average AoI is minimized when the packet rate p is close to 0.011. With the increase in packet rate p , the CSMA/CA based network performs better than the slotted ALOHA based network. Third, we observe that the Monte Carlo simulation results and theoretical results of the slotted ALOHA based network match well while the Monte Carlo simulation results and theoretical results of the CSMA/CA based network slightly diverges when $p > 0.013$. For the CSMA/CA protocol, the mismatch between analysis and simulation is because the distribution of the real service time deviates from the geometric distribution as the packet rate and the number of nodes increase.

Fig. 7(b) presents how the average AoIs of the networks change with the number N of the sensor node when the packet rate is set to $p = 0.01$. As is shown, the average AoI is increasing with the number N of the sensor nodes. This is because

as the population of nodes grows, the frequency of collisions becomes larger, and the service time would also be longer. In particular, the change in the average AoI of the CSMA/CA based network is relatively flat compared to the change in the average AoI of the slotted ALOHA based network. We also observe that the performance of the CSMA/CA based network is better than the slotted ALOHA based network as the number N of sensor nodes is increased. Moreover, it is seen from Fig. 7(b) that the Monte Carlo simulation results of the slotted ALOHA based network match well with the theoretical results, while the Monte Carlo simulation results of the CSMA/CA based network deviate slightly from the theoretical results when $N > 24$.

From Figs. 7(a) and 7(b), we also see that the average AoI of the CSMA/CA based network is always smaller than that of the slotted ALOHA based network, regardless of the

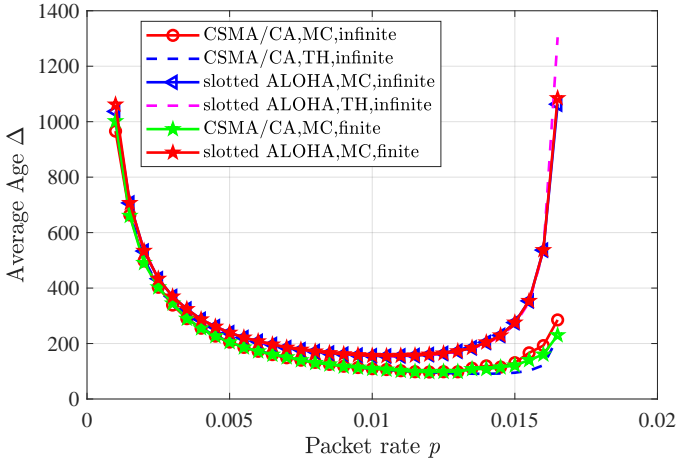
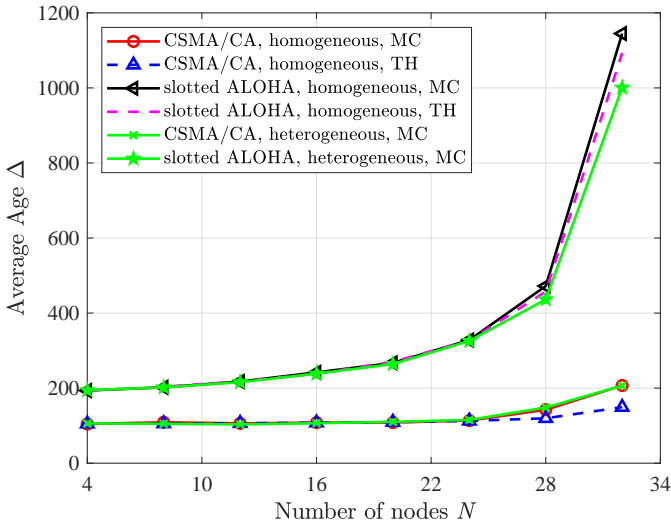
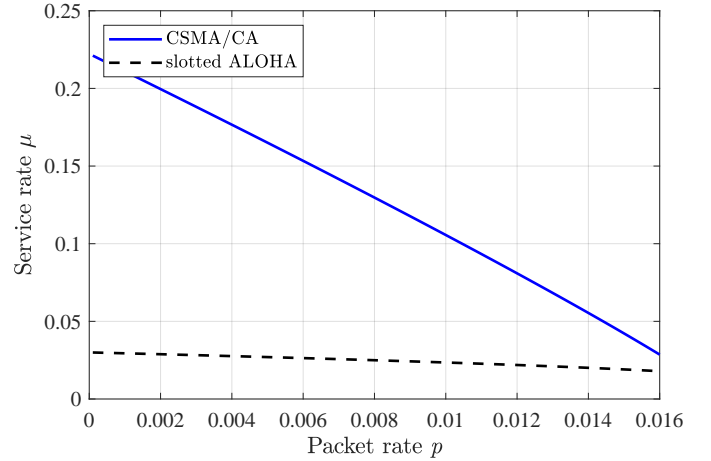
(a) Average AoI versus the packets packet rate p ($N = 20$ and $\lambda = 0.03$)(b) Average AoI versus the number of the nodes N ($p = 0.01$ and $\lambda = 0.0186$)

Fig. 7. Change in the average AoI.

packet rate p and the number N of nodes. Note that for comparison fairness, the attempt probability λ of the slotted ALOHA protocol is chosen in such a way that the transmission probabilities of the two scheme are equal for given the packet rate p . For example, we have $\lambda = 0.03$ when the number of sensor nodes is set to $N = 20$; we have $\lambda = 0.0186$ when the packet rate is set to $p = 0.01$. From (13) and (24), it is clear that the collision probabilities p_{cl} of the two networks using the CSMA/CA protocol and the slotted ALOHA protocol are equal when their transmission probabilities p_{tx} are the same. According to Theorem 2, we can see that the average AoI of the network is related to the packet rate p and the service rate μ . For a given same packet rate p case, it is the service rate that determines the average AoI of the network. Therefore, the difference in network performance by using the CSMA/CA

Fig. 8. Service rate μ versus packet rate p .

protocol and the slotted ALOHA protocol AoI comes from their different service rates. We observe from Fig. 8 that the service rate of the network using the CSMA/CA protocol is always much larger than that of the slotted ALOHA protocol. From Fig. 8 and Theorem 2, the difference in AoI performance when the network uses these two protocols can be explained. This suggests that CSMA/CA is superior to slotted ALOHA systems and maybe is the most promising mode in the design of WSN systems.

In addition, we investigate how the average AoI varies with packet rate p in the finite buffer and finite retransmission cases (for CSMA, i.e., the maximum number of back-off stages) through Monte Carlo simulations, in which the buffer size is set to 30 packets, the number of retransmission is set to 8, and we use ‘finite’ to denote finite buffers and retransmission. It is observed from Fig. 7(a) that the average AoI with packet rate p for the finite buffer and retransmission cases remains consistent with that for the infinite buffer and retransmission cases. That is, a 30 packets buffer and 8 retransmissions are enough for the network.

In practical wireless sensor networks, since the data packet generation rates of the sensor nodes are not necessarily the same, we also study the performance of heterogeneous networks by Monte Carlo simulations. That is, the packet rates of the nodes are different from each other. In particular, the packet rates of the nodes are randomly chosen in a finite range $[0, 2p_{max}]$ while ensuring their average is equal to the packet rate p of the corresponding homogeneous network. From Figs. 5(b), 6(b) and 7(b), the changes in transmission probability p_{tx} , the collision probability p_{cl} , and the average AoIs are with similar modes to the corresponding homogeneous networks.

V. CONCLUSION

In this paper, we investigated the timeliness of two wireless sensor networks using the CSMA/CA protocol and the slotted ALOHA protocol. We showed that the average AoI would

be larger when the packet rate is small or relatively large. With the same transmission probability, the average AoI of the network employing the CSMA/CA protocol is always smaller than that one using the slotted ALOHA protocol, irrespective of the packet rate and the growth in the number of nodes. In addition, we also found that the effects of variation of the transmission probability p_{tx} , the collision probability p_{cl} , and the average AoIs of the heterogeneous networks are basically similar to that in the homogeneous networks. It is noted that the limitation of methods developed in this paper assumes that each update takes one slot. In future work, we shall consider where multiple slots are required for each update and there exist some hidden nodes.

APPENDIX

A. Proof of Proposition 1

Proof. First, for a given data packet arrival rate $p < \mu_{\text{CA}}$, it is clear that each data packet in the node buffer will be successfully delivered within a certain period. Especially, in the zeroth back-off stage, the back-off counter will definitely return to zero eventually and stay at state $(0, 0, k)$ for some $k \geq 1$ for exactly one slot. Therefore, we have $b_{0,0,*} = p$.

Second, a state will transfer from the $(i, 0, *)$ to the $(i+1)$ th back-off stage if a collision occurs in the current slot. In this case, the state returns to and stays at state $(i+1, 0)$ for exactly one slot, and thus we have

$$b_{i,0,*}p_{\text{cl}} = b_{i+1,0,*}, \quad (39)$$

in which $i \geq 0$. Further, we have

$$b_{i,0,*} = p_{\text{cl}}^i b_{0,0,*} = pp_{\text{cl}}^i, \quad (40)$$

in which $i \geq 0$. In fact, we are able to use the dynamic equilibrium property of the stationary Markov chains to prove the (40). To this end, we shall divide the state space into two parts: The states (i', j, k) with $i' \leq i$ and the states (i'', j, k) with $i'' \geq i$. Since the total transiting probability from the left part to right part is equal to the total transiting probability from the right part to the left part, thus we have

$$\begin{aligned} b_{i,0,*}p_{\text{cl}} &= \sum_{i''=i+1}^{\infty} b_{i'',0,*}(1-p_{\text{cl}}) \\ &= b_{i+1,0,*}(1-p_{\text{cl}}) + \sum_{i''=i+2}^{\infty} b_{i'',0,*}(1-p_{\text{cl}}), \end{aligned} \quad (41)$$

which yields

$$b_{i+1,0,*}p_{\text{cl}} = \sum_{i''=i+2}^{\infty} b_{i'',0,*}(1-p_{\text{cl}}). \quad (42)$$

By combining (41) with (42), (39) can be obtained readily.

We denote the initial back-off counter of the i -th back-off stage as J and have

$$\Pr\{J \geq j\} = \frac{w_i - j}{w_i}, \quad (43)$$

in which $0 \leq j \leq w_i - 1$. We know that a node has a opportunity to stay at state $(i, j, *)$ only if the initial back-off counter J is no less than j . As the back-off counter has

been decreased to j , the expected sojourn time at the state would be

$$\bar{L} = \sum_{l=1}^{\infty} l(1-p_{\text{cl}})p_{\text{cl}}^{l-1} = \frac{1}{1-p_{\text{cl}}}. \quad (44)$$

Afterwards, the state eventually transits to the state $(i, 0, *)$ and stay for exactly one slot. Therefore, the stationary probability for the node to be in state $(i, j, *)$ can be expressed as

$$b_{i,j,*} = \bar{L} \Pr\{J \geq j\} b_{i,0,*} = \frac{p(w_i - j)p_{\text{cl}}^i}{w_i(1-p_{\text{cl}})}, \quad (45)$$

in which $i \geq 0$, $0 \leq j \leq w_i - 1$, and we use (39). Moreover, we also can apply the dynamic equilibrium equation to the Markov chain to prove (45).

Finally, by the normalized condition of the stationary distribution, we have

$$\begin{aligned} b_{-1} &= b_{-1,-1,0} = 1 - \sum_{i=0}^{\infty} b_{i,0,*} - \sum_{i=0}^{\infty} \sum_{j=1}^{w_i-1} b_{i,j,*} \\ &= 1 - \sum_{i=0}^{\infty} pp_{\text{cl}}^i - \sum_{i=0}^{\infty} \frac{pp_{\text{cl}}^i}{1-p_{\text{cl}}} \sum_{j=1}^{w_i-1} \left(1 - \frac{j}{w_i}\right) \\ &= 1 - \frac{p(4p_{\text{cl}}^2 - (w_0 + 4)p_{\text{cl}} + w_0 + 1)}{2(1-p_{\text{cl}})^2(1-2p_{\text{cl}})}. \end{aligned} \quad (46)$$

This completes the proof of the Proposition 1. \blacksquare

B. Proof of Theorem 1

Proof. Based on Proposition 1 and the fact that every attempted transmission occurs when the back-off counter is zero, the transmission probability p_{tx} can be expressed as

$$p_{\text{tx}} = \sum_{i=0}^{\infty} b_{i,0,*} = \sum_{i=0}^{\infty} p_{\text{cl}}^i b_{0,0,*} = \frac{p}{1-p_{\text{cl}}}. \quad (47)$$

It is seen from (47) that the transmission probability p_{tx} depends on the collision probability p_{cl} , which is also unknown. To address the unknown collision probability, it is worth noting that the collision probability refers to the probability that at least one of the remaining $N - 1$ nodes in the same slot will interfere. Consequently, the collision probability p_{cl} can be expressed by the transmission probability p_{tx} ,

$$p_{\text{cl}} = 1 - (1 - p_{\text{tx}})^{N-1}, \quad (48)$$

in which, p_{tx} is the transmission probability of the data packets, $(1 - p_{\text{tx}})$ is the non-transmission probability of the data packets, $(1 - p_{\text{tx}})^{N-1}$ is the probability that none of the remaining $N - 1$ nodes transmits, and $(1 - (1 - p_{\text{tx}})^{N-1})$ is the probability that at least one of the remaining $N - 1$ nodes transmits, i.e., the collision probability p_{cl} .

This completes the proof of the Theorem 1. \blacksquare

C. Proof of Proposition 2

Proof. According to the state transition diagram of the discrete-time Markov chain given in Fig. 4, when the steady-

state is reached, the transfer in is equal to the transfer out, we have the following balance equations

$$\begin{cases} pb_0 = \mu_{SA}\bar{p}b_1 \\ pb_0 + \mu_{SA}\bar{p}b_2 = (p\bar{\mu}_{SA} + \mu_{SA}\bar{p})b_1 \\ p\bar{\mu}_{SA}b_{k-1} + \mu_{SA}\bar{p}b_{k+1} = (p\bar{\mu}_{SA} + \mu_{SA}\bar{p})b_k, \quad k \geq 2, \end{cases} \quad (49)$$

in which, $\bar{p} = 1 - p$, $\bar{\mu}_{SA} = 1 - \mu_{SA}$. It is assumed that b_0 is a undetermined constant.

From (49), we further obtain

$$b_1 = \frac{p}{\mu_{SA}(1-p)}b_0, \quad (50)$$

$$b_2 = \frac{p^2(1-\mu_{SA})}{\mu_{SA}^2(1-p)^2}b_0, \quad (51)$$

$$b_3 = \frac{p^3(1-\mu_{SA})^2}{\mu_{SA}^3(1-p)^3}b_0. \quad (52)$$

Thus, it is concluded that

$$b_k = \frac{p^k(1-\mu_{SA})^{k-1}}{\mu_{SA}^k(1-p)^k}b_0 \quad (53)$$

$$= \frac{p}{\mu_{SA}(1-p)} \frac{(p(1-\mu_{SA}))^{k-1}}{(\mu_{SA}(1-p))^{k-1}}b_0, \quad k \geq 1. \quad (54)$$

Moreover, we know that the sum of total probabilities is equal to one, i.e.,

$$\sum_{k=0}^{\infty} b_k = 1. \quad (55)$$

By substituting (53) into (55), we have

$$b_0 + \frac{p}{\mu_{SA}(1-p)}b_0 \sum_{k=1}^{\infty} \frac{(p(1-\mu_{SA}))^{k-1}}{(\mu_{SA}(1-p))^{k-1}} = 1. \quad (56)$$

In order to maintain the stability of the system, the rate of the packets generation must be no longer than the mean service rate, i.e., $p < \mu_{SA}$. Thus, we have

$$\frac{p(1-\mu_{SA})}{\mu_{SA}(1-p)} < 1. \quad (57)$$

According to (56) and (57), b_0 can be expressed by the following expression

$$b_0 = \frac{\mu_{SA} - p}{\mu_{SA}} = 1 - \frac{p}{\mu_{SA}}, \quad (58)$$

in which b_0 is the probability that the buffer is empty.

Thus, the proof of Proposition 2 has been accomplished. ■

D. Proof of Theorem 2

Proof. Since as M approaches infinity, A_0 and $T_k(T_k + 1)/2$ are finite with respect to $\sum_{k=1}^{K-1} A_k$, A_0 and $T_k(T_k + 1)/2$ could be neglected. Therefore, the average AoI (cf. (4)) could be rewritten as

$$\bar{\Delta} = \lim_{M \rightarrow \infty} \frac{1}{M} \sum_{k=1}^{K-1} A_k$$

$$\begin{aligned} &= \lim_{M \rightarrow \infty} \frac{k-1}{M} \frac{1}{k-1} \sum_{k=1}^K A_k \\ &= p\mathbb{E}[A_k], \end{aligned} \quad (59)$$

in which $p = \lim_{M \rightarrow \infty} K/M$ is the rate of node state update generation (packet arrival rate) and $\mathbb{E}[\cdot]$ is the expectation operator. In addition, we could use the inter-arrival time X_k and the system time T_k to represent the average area of A_k , as shown in the following expression.

$$\begin{aligned} \mathbb{E}[A_k] &= \mathbb{E}\left[\sum_{m=1}^{X_k+T_k} m\right] - \mathbb{E}\left[\sum_{m=1}^{T_k} m\right] \\ &= \frac{1}{2}\mathbb{E}[(X_k+T_k)(X_k+T_k+1)] - \frac{1}{2}\mathbb{E}[T_k(T_k+1)] \\ &= \frac{1}{2}\mathbb{E}[X_k^2] + \frac{1}{2}\mathbb{E}[X_k] + \mathbb{E}[X_kT_k]. \end{aligned} \quad (60)$$

Since the generation of packets (the arrivals of packets) is a Bernoulli process with rate p , the probability distribution of the inter-arrival time X_k of a packet would be $\Pr\{X_k = j\} = p(1-p)^{j-1}$, $j = 1, 2, \dots$. Therefore, the first and second moments of the inter-arrival time X_k of a packet are given, respectively, by

$$\mathbb{E}[X_k] = \frac{1}{p}, \quad (61)$$

$$\mathbb{E}[X_k^2] = \frac{2-p}{p^2}. \quad (62)$$

Note that in (60), the only part is $\mathbb{E}[X_kT_k]$ unknown. Furthermore, when the k th update arrives, the waiting time W_k is equal to zero if the $k-1$ update has completed the service, and it is $T_{k-1} - X_k$ if the $k-1$ update is being served or waiting. Therefore, we have $W_k = \max(T_{k-1} - X_k, 0)$. Because the inter-arrival time X_k and the service time S_k are independent of one another while the inter-arrival time X_k and the waiting time W_k are related with each other, $\mathbb{E}[X_kT_k]$ could be written as (cf. (2))

$$\begin{aligned} \mathbb{E}[X_kT_k] &= \mathbb{E}[X_k(W_k + S_k)] \\ &= \mathbb{E}[X_kW_k] + \mathbb{E}[X_k]\mathbb{E}[S_k]. \end{aligned} \quad (63)$$

In order to obtain $\mathbb{E}[X_kW_k]$, we introduce the auxiliary function $H(z)$ as follows (cf. [34])

$$\begin{aligned} H(z) &= \sum_{i=1}^{\infty} z^i \Pr\{X_k = i\} \sum_{j=0}^{\infty} \Pr\{T_{k-1} > i + j\} \\ &= \sum_{i=1}^{\infty} z^i \Pr\{X_k = i\} \sum_{j=i}^{\infty} \Pr\{T_{k-1} > j\} \\ &= \sum_{i=1}^{\infty} z^i p(1-p)^{i-1} \frac{(1-\beta)^i}{\beta} \\ &= \frac{p(1-\beta)z}{\beta(1-(1-p)(1-\beta)z)}, \end{aligned} \quad (64)$$

where

$$\Pr\{T_{k-1} > j\} = 1 - \Pr\{T_{k-1} \leq j\}$$

$$\begin{aligned}
&= 1 - \sum_{l=1}^j \beta(1-\beta)^{l-1} \\
&= (1-\beta)^j.
\end{aligned} \tag{65}$$

Moreover, $\mathbb{E}[X_k W_k]$ can be represented as

$$\begin{aligned}
\mathbb{E}[X_k W_k] &= \mathbb{E}[X_k \max(0, T_{k-1} - X_k)] \\
&= \sum_{i=1}^{\infty} i \Pr\{X_k = j\} \sum_{j=0}^{\infty} \Pr\{\max(0, T_{k-1} - i) > j\} \\
&= \sum_{i=1}^{\infty} i \Pr\{X_k = j\} \sum_{j=0}^{\infty} \Pr\{T_{k-1} > i + j\} \\
&= \lim_{z \rightarrow 1^-} (H(z))' \\
&= \lim_{z \rightarrow 1^-} \frac{p(1-\beta)}{\beta} \\
&\quad \times \frac{(1 - (1-p)(1-\beta)z + z(1-p)(1-\beta))}{(1 - (1-p)(1-\beta)z)^2} \\
&= \frac{p(1-\beta)}{\beta(1 - (1-p)(1-\beta))^2}.
\end{aligned} \tag{66}$$

By replacing β in (66) with (35), we further have

$$\mathbb{E}[X_k W_k] = \frac{p(1-\mu)}{(\mu-p)\mu^2}. \tag{67}$$

According to (59) to (63) and (67), the average AoI can be expressed as

$$\begin{aligned}
\bar{\Delta} &= p\mathbb{E}[A_k] \\
&= p \left[\frac{1}{2}\mathbb{E}[X_k] + \frac{1}{2}\mathbb{E}[X_k^2] + \mathbb{E}[X_k]\mathbb{E}[S_k] + \mathbb{E}[X_k W_k] \right] \\
&= p \left[\frac{1}{2p} + \frac{2-p}{2p^2} + \frac{1}{p\mu} + \frac{p(1-\mu)}{(\mu-p)\mu^2} \right] \\
&= \frac{1}{p} + \frac{p}{\mu} + \frac{1-p}{\mu-p} - \frac{p}{\mu^2}.
\end{aligned} \tag{68}$$

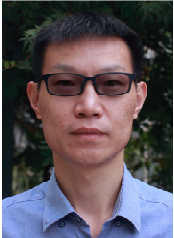
Thus, the proof of Theorem 2 has been completed. ■

REFERENCES

- [1] H. Habibzadeh *et al.*, "A Survey of healthcare Internet of Things (HIoT): A clinical perspective," *IEEE Internet Things J.*, vol. 7, no. 1, pp. 53–71, Jan. 2020.
- [2] B. V. Philip, T. Alpcan, J. Jin, and M. Palaniswami, "Distributed real-time iot for autonomous vehicles," *IEEE Trans. Ind. Informat.*, vol. 15, no. 2, pp. 1131–1140, Feb. 2019.
- [3] S. Chaudhary, R. Johari, R. Bhatia, K. Gupta, and A. Bhatnagar, "CRAIoT: Concept, review and application(s) of IoT," in *Proc. IoT-SIU*, 2019.
- [4] S. Kaul, M. Gruteser, V. Rai, and J. Kenney, "Minimizing age of information in vehicular networks," in *Proc. IEEE SECON*, 2011.
- [5] S. Kaul, R. Yates, and M. Gruteser, "Real-time status: How often should one update?," in *Proc. IEEE INFOCOM*, 2012.
- [6] J. P. Champati, H. Al-Zubaidy, and J. Gross, "Statistical guarantee optimization for age of information for the D/G/1 queue," in *Proc. IEEE INFOCOM*, 2018.
- [7] A. Soysal and S. Ulukus, "Age of information in G/G/1/1 systems: Age expressions, bounds, special cases, and optimization," *IEEE Trans. Inf. Theory*, vol. 67, no. 11, pp. 7477–7489, Nov. 2021.
- [8] S. K. Kaul, R. D. Yates, and M. Gruteser, "Status updates through queues," in *Proc. CISS*, 2012.
- [9] A. M. Bedewy, Y. Sun, and N. B. Shroff, "Optimizing data freshness, throughput, and delay in multi-server information-update systems," in *Proc. IEEE ISIT*, 2016.
- [10] Y. Sun, E. Uysal-Biyikoglu, R. D. Yates, C. E. Koksal, and N. B. Shroff, "Update or wait: How to keep your data fresh," *IEEE Trans. Inf. Theory*, vol. 63, no. 11, pp. 7492–7508, Nov. 2017.
- [11] G. Bianchi, "Performance analysis of the IEEE 802.11 distributed coordination function," *IEEE J. Sel. Areas in Commun.*, vol. 18, no. 2, pp. 535–547, Mar. 2000.
- [12] K. Duffy, D. Malone, and D. J. Leith, "Modeling the 802.11 distributed coordination function in non-saturated conditions," *IEEE Commun. Lett.*, vol. 9, no. 8, pp. 715–717, Aug. 2005.
- [13] B. S. Tsybakov and V. A. Mikhailov, "Ergodicity of a slotted ALOHA system," *Probl. Inf. Transm.*, vol. 15, no. 4, pp. 73–87, 1979.
- [14] S. Ghez, S. Verdu, and S. C. Schwartz, "Stability properties of slotted ALOHA with multipacket reception capability," *IEEE Trans. Autom. Control*, vol. 33, no. 7, pp. 640–649, Jul. 1988.
- [15] M. Wang and Y. Dong, "Broadcast age of information in CSMA/CA based wireless networks," in *Proc. IEEE ACM IWCMC*, 2019.
- [16] A. Maatouk, M. Assaad, and A. Ephremides, "On the age of information in a CSMA environment," *IEEE/ACM Trans. Netw.*, vol. 28, no. 2, pp. 818–831, Apr. 2020.
- [17] A. Maatouk, M. Assaad, and A. Ephremides, "Minimizing the age of information in a CSMA environment," in *Proc. WiOPT*, 2019.
- [18] M. Moltafet, M. Leinonen, and M. Codreanu, "Worst case age of information in wireless sensor networks: A multi-access channel," *IEEE Wireless Commun. Lett.*, vol. 9, no. 3, pp. 321–325, Mar. 2020.
- [19] L. Li, Y. Dong, C. Pan, and P. Fan, "Age of information of CSMA/CA based wireless networks," in *Proc. IEEE ACM IWCMC*, 2022.
- [20] M. O'Kennedy, T. Niesler, R. Wolhuter, and N. Mitton, "Practical evaluation of carrier sensing for a LoRa wildlife monitoring network," in *Proc. IFIP Networking Conf. (Networking)*, 2020.
- [21] C. Pham, "Investigating and experimenting CSMA channel access mechanisms for LoRa IoT networks," in *Proc. IEEE WCNC*, 2018.
- [22] R. D. Yates and S. K. Kaul, "Status updates over unreliable multi-access channels," in *Proc. IEEE ISIT*, Aachen, Germany, Jun. 2017, pp. 331–335.
- [23] X. Chen, K. Gatsis, H. Hassani, and S. S. Bidokhti, "Age of information in random access channels," in *Proc. IEEE ISIT*, 2020.
- [24] I. Kadota, A. Sinha, and E. Modiano, "Scheduling algorithms for optimizing age of information in wireless networks with throughput constraints," *IEEE/ACM Trans. Netw.*, vol. 27, no. 4, pp. 1359–1372, Aug. 2019.
- [25] R. D. Yates and S. K. Kaul, "Age of information in uncoordinated unslotted updating," in *Proc. IEEE ISIT*, 2020.
- [26] A. Munari, "On the value of retransmissions for age of information in random access networks without feedback," Available: <https://doi.org/10.48550/arXiv.2205.15077>.
- [27] H. Chen, Y. Gu, and S.-C. Liew, "Age-of-information dependent random access for massive IoT networks," in *Proc. IEEE INFOCOM*, 2020.
- [28] O. T. Y. avascan and E. Uysal, "Analysis of slotted ALOHA with an age threshold," *IEEE J. Sel. Areas Commun.*, vol. 39, no. 5, pp. 1456–1470, May 2021.
- [29] J. T. Lim and Y. Han, "Spreading factor allocation for massive connectivity in LoRa systems," *IEEE Commun. Lett.*, vol. 22, no. 4, pp. 800–803, Apr. 2018.
- [30] M. de Castro Tom, P. H. J. Nardelli, and H. Alves, "Long-range low-power wireless networks and sampling strategies in electricity metering," *IEEE Trans. Ind. Electron.*, vol. 66, no. 2, pp. 1629–1637, Feb. 2019.
- [31] Y. A. Al-Gumaei, N. Aslam, X. Chen, M. Raza, and R. I. Ansari, "Optimizing power allocation in LoRaWAN IoT applications," *IEEE Internet Things J.*, vol. 9, no. 5, pp. 3429–3442, March, 2022.
- [32] Q. Li and N. Wang, *Numerical analysis*, Tsinghua University Press, Beijing, China, 2008.
- [33] N. Tian and X. Xu, *Discrete time queuing theory*, Science Press, Beijing, China, 2008.
- [34] Y. Dong, Z. Chen, and P. Fan, "Timely two-way data exchanging in unilaterally powered fog computing systems," *IEEE Access*, vol. 7, pp. 21103–21117, 2019.



Liang Li received the B.S. degree in Communication Engineering from Nanjing University of Information Science and Technology, Nanjing, China, in 2020, and he is currently pursuing the M.S. degree in Electronic Information from Nanjing University of Information Science and Technology. His research interests include the performance evaluations of wireless networks and age of information.



Yunquan Dong (M'15) received the B.S. degree in Electronic and Information Engineering from Qingdao University in 2005, the M.S. degree in Communication and Information Systems from Beijing University of Posts and Telecommunications 2008, and the Ph.D. degree in Communication and Information Engineering from Tsinghua University, Beijing, in 2014.

He was a BK Assistant Professor with the Department of Electrical and Computer Engineering, Seoul National University, Seoul, South Korea, from

2015 to 2016. He is currently a Professor with the School of Electronic and Information Engineering, Nanjing University of Information Science and Technology, Nanjing, China. His research interests include the performance evaluations and performance optimizations of wireless networks, with recent focus on age of information and ubiquitous sensing.



Chengsheng Pan received the B.S. and M.S. degrees from Nanjing University of Science and Technology, in 1984 and 1987, respectively, and the Ph.D. degree from Northeastern University, in 2001. Since 1989, he has been an Assistant Professor with Shenyang Ligong University. He is currently a Professor with the Nanjing University of Information Science and Technology and a part-time Ph.D. advisor with the Nanjing University of Science and Technology. He has authored three books and more than 150 articles. His research interests include

intelligent network traffic theory and key technologies.



Pingyi Fan (M'03-SM'09) received the B.S. degree from the Department of Mathematics, Hebei University, in 1985, the M.S. degree from Nankai University in 1990, and the Ph.D. degree from the Department of Electronic Engineering, Tsinghua University, Beijing, China, in 1994.

From August 1997 to March 1998, he visited the Hong Kong University of Science and Technology as a Research Associate. From May 1998 to October 1999, he visited the University of Delaware, USA, as a Research Fellow. In March 2005, he visited NICT,

Japan, as a Visiting Professor. From June 2005 to May 2014, he visited The Hong Kong University of Science and Technology many times. From July 2011 to September 2011, he was a Visiting Professor with the Institute of Network Coding, The Chinese University of Hong Kong. He is currently a Professor with the Department of EE, Tsinghua University. His main research interests include 5G technology in wireless communications, such as MIMO, OFDMA, network coding, network information theory, machine learning, and big data analysis.

Dr. Fan is an Overseas Member of IEICE. He has received some academic awards, including the IEEE WCNC08 Best Paper Award, the ACM IWCMC10 Best Paper Award, the IEEE Globecom14 Best Paper Award, the IEEE ICC20 Best Paper Award, the IEEE TAOS Technical Committee20 Best Paper Award, and the CIEIT Best Paper Awards in 2018 and 2019. Also, he has received the IEEE ComSoc Excellent Editor Award for IEEE TRANSACTIONS ON WIRELESS COMMUNICATIONS in 2009. He has attended to organize many international conferences, including as the General Co-Chair of EAI Chinacom 2020 and IEEE VTS HMWC 2014, the TPC Co-Chair of IEEE International Conference on Wireless Communications, Networking and Information Security (WCNIS 2010), and the TPC Member of IEEE ICC, GLOBECOM, WCNC, VTC, and INFOCOM. He is also a Reviewer of more than 30 international journals, including 20 IEEE journals and eight EURASIP journals. He has served as an Editor for IEEE TRANSACTIONS ON WIRELESS COMMUNICATIONS, International Journal of Ad Hoc and Ubiquitous Computing (Inderscience), journal of Wireless Communications & Mobile Computing (Wiley), Electronics (MDPI), and Open Journal of Mathematical Sciences.